GEOMETRIC TRANSFORMATIONS IN DESIGNING NEW MATERIALS

LIGIA MUNTEANU*, DAN DUMITRIU*, VETURIA CHIROIU*

Abstract. In this paper, an original idea of designing new materials is investigated. The property of Helmholtz equation to be invariant under geometric transformations is exploited to obtain new materials with inhomogeneous and anisotropic distribution of elastic properties. This approach opens up the possibility to configure new materials that might be useful in the design of elastic cloaking devices.

Key words: geometric transformations, material design, Helmholtz equation, invariant, cloaking devices.

1. INTRODUCTION

Over the last two decades a new field has emerged which is concerned with acoustic metamaterials which could cloak regions of space, making them invisible to sound [9, 11, 18]. We refer to acoustic cloaking which occurs when a medium contains a region in which noisy objects can be acoustically hidden. It is easy to imagine an object invisible to sound by building a box around it to prevent the wave from reaching the object.

The idea for transforming homogeneous and isotropic materials into new inhomogeneous and anisotropic materials is the focus of this paper, mainly based on the geometric transformations.

This idea is related to the current research in invisibility cloaks starting from the works of Pendry, Schurig and Smith [18] (cloaking via changes of coordinates), Leonhardt [11] (cloaking via conformal mapping), Milton and Nicorovici [12] (cloaking by reaction), Alu and Engheta [1] (plasmonic cloaking), Greenleaf, Lassas and Uhlmann [8] (cloaking in inverse problems), Milton [13] (elastic metamaterials) and Munteanu and Chiroiu [15] (acoustic cloaking).

Milton, Briane and Willis [14] showed that geometric transformations cannot be applied to equations which are not invariant under coordinate transformations and, consequently, if cloaking exists for such equations (for example the elasticity equations), it would be of a different nature from acoustic and electromagnetic.

However, the crucial point of Brun, Guenneau and Movchan [3] is that the Navier equations are not unchanged unless one allows the symmetries of the elasticity tensor to be violated. The aforementioned authors derive the elastic

* Institute of Solid Mechanics of the Romanian Academy, Ctin Mille 15, Bucharest 010141, Romania; E-mails: ligia_munteanu@hotmail.com, dumitri04@yahoo.com, veturiachiroiu@yahoo.com

Rev. Roum. Sci. Techn. – Méc. Appl., Tome 56, Nº 3, P. 272–284, Bucarest, 2011

properties of a cylindrical cloak for in-plane coupled shear and pressure waves. The cloak is characterized by a rank 4 elasticity tensor with spatially varying entries, which are deduced from a geometric transform. Remarkably, the Navier equations retain their form under this transform, which is generally untrue [12]. Further details on this point can be found in [17, 27].

The paper is organized as follows: §2 is devoted to the geometric transformations. The idea is to replace the initial material (homogeneous and isotropic) in the initial domain by an equivalent transformed domain that contains a new inhomogeneous (the properties are no longer constants but depend on coordinates) and anisotropic (tensorial nature) material.

A challenge to the plausibility of applying the geometric transformations for designing new materials is the aim of §3. Concluding remarks are provided in §4.

2. GEOMETRIC TRANSFORMATIONS

Pendry, Shurig and Smith [18] proved that a finite size object surrounded by a coating consisting of a specially designed metamaterial would become invisible for electromagnetic waves at any frequency. The idea is that the sound sees the space differently [7]. For the sound, the concept of distance is modified by the acoustic properties of the regions through which the sound travels. In geometrical acoustics, the idea of the acoustical path when travelling an infinitesimal distance $\mathrm{d}s$, is the corresponding acoustical path length $c^{-1}\mathrm{d}s$, where $c^{-1}=\sqrt{\rho/\kappa}$ with ρ the fluid density and κ the compression modulus of the fluid. Cummer and Schurig [5] demonstrated that acoustic waves in a fluid undergo the same geometric transformation as electromagnetic waves do and therefore retain their form. For example, the 3D equation for the pressure waves propagating in a bounded fluid region $\Omega\subset \mathrm{R}^3$ is the Helmholtz equation

$$\nabla\cdot(\underline{\underline{\rho}}^{-1}\nabla p)+\frac{\omega^2}{\kappa}p=0, \tag{1}$$

where p is the pressure, $\underline{\underline{\rho}}$ is the rank-2 tensor of the fluid density, κ is the compression modulus of the fluid and ω is the wave frequency.

Geometric transformations applied to certain types of elastodynamic waves in structural mechanics received less attention, since the Navier equations do not usually retain their form under geometric changes [2, 16]. For example, the in-plane propagation of time-harmonic elastic waves is governed by the Navier equations

$$\nabla\cdot C:\nabla U+\rho\omega^2 U+b=0, \tag{2}$$

where u is the displacement, ρ the density, C the 4th-order material tensor of the linear elastic material and $b(x)$ represents the spatial distribution of a simple harmonic body force: $b(x,t)=b(x)\exp(\mathrm{i}\omega t)$, with ω the wave-frequency and t the time.

Let us consider the geometric transformation from the coordinate system (x',y',z') of the compressed space to the original coordinate system (x,y,z), given by $x(x',y',z')$, $y(x',y',z')$ and $z(x',y',z')$. The change of coordinates is characterized by the transformation of the differentials through the Jacobian $J_{xx'}$ of this transformation, *i.e.*

$$\begin{pmatrix} \mathrm{d}x \\ \mathrm{d}y \\ \mathrm{d}z \end{pmatrix} = J_{xx'} \begin{pmatrix} \mathrm{d}x' \\ \mathrm{d}y' \\ \mathrm{d}z' \end{pmatrix}, \quad J_{xx'} = \frac{\partial(x,y,z)}{\partial(x',y',z')} . \tag{3}$$

From the geometrical point of view, the change of coordinates implies that, in the transformed region, one can work with an associated metric tensor [9,28]:

$$T = \frac{J_{xx'}^{\mathrm{T}} J_{xx'}}{\det(J_{xx'})} . \tag{4}$$

In terms of the material parameters, one can replace the material from the original domain (homogeneous and isotropic) by an equivalent compressed one that is inhomogeneous (its characteristics depend on the spherical (r',θ',ϕ') coordinates) and anisotropic (described by a tensor), and whose properties, in terms of $J_{x'x}$, are given by

$$\underline{\underline{\rho}}' = J_{x'x}^{-\mathrm{T}}\, \rho\, J_{x'x}^{-1} \det(J_{x'x}), \quad \kappa' = \kappa \det(J_{x'x}), \tag{5}$$

or, equivalently, in terms of $J_{xx'}$:

$$\underline{\underline{\rho}}' = \frac{J_{xx'}^{\mathrm{T}}\, \rho\, J_{x'x}}{\det(J_{xx'})}, \quad \kappa' = \frac{\kappa}{\det(J_{xx'})} . \tag{6}$$

Here, $\underline{\underline{\rho}}'$ is a second order tensor. When the Jacobian matrix is diagonal, equations (5) and (6) can be more easily written. Multiplying (1) by a test function φ and integrating by parts, one obtains [7]:

$$-\int_{\Omega} \left(\nabla_{(x,y,z)}\varphi \cdot \underline{\underline{\rho}}^{-1} \nabla_{(x,y,z)} p \right) \mathrm{d}V + \int \left(\omega^2 \kappa^{-1} p \varphi \right) \mathrm{d}V = 0 . \tag{7}$$

In (7) the surface integral, corresponding to a Neumann integral over the boundary $\partial\Omega$, is zero. By applying the coordinate transformation $(x,y,z)\to(x',y',z')$ to (7) and using (3), one obtains

$$-\int_{\Omega}\left(J_{x'x}^{\mathrm{T}}\nabla_{(x',y',z')}\varphi\cdot\underline{\underline{\rho}}^{-1}J_{x'x}^{\mathrm{T}}\nabla_{(x,y,z)}p\right)\det(J_{xx'})\mathrm{d}V'+\int\left(\det(J_{xx'})\omega^{2}\kappa^{-1}p\varphi\right)\mathrm{d}V'=0\,, \tag{8}$$

in terms of $J_{xx'}$, and

$$-\int_{\Omega}\left(\left(\nabla_{(x',y',z')}\varphi\right)^{\mathrm{T}}\frac{J_{x'x}\underline{\underline{\rho}}^{-1}J_{x'x}^{\mathrm{T}}}{\det(J_{x'x})}\nabla_{(x',y',z')}p\right)\mathrm{d}V'+\int\left(\frac{\kappa^{-1}}{\det(J_{x'x})}\omega^{2}p\varphi\right)\mathrm{d}V'=0\,, \tag{9}$$

in terms of $J_{x'x}$.

A linear geometric transformation (3) which maps the disk $r\le R_2$ into an annulus $R_1\le r\le R_2$ [18] is given by:

$$\begin{gathered} r'=R_1+r\frac{R_2-R_1}{R_2},\ \ 0\le r\le R_2\,,\\ \theta'=\theta,\ \ 0\le\theta\le 2\pi\,,\\ x_3'=x_3,\ \ \ x_3\in\mathrm{R}\,, \end{gathered} \tag{10}$$

where r', θ', x_3' are radially contracted cylindrical coordinates r, θ, x_3. The Cartesian basis (x_1,x_2,x_3) is defined as $x_1=r\cos\theta$, $x_2=r\sin\theta$. The Jacobean of the transformation from polar to stretched polar coordinates is given by $J_{rr'}=\dfrac{\partial(r,\theta,x_3)}{\partial(r',\theta',x_3')}$. In the stretched space, the associated metric tensor is given by (4):

$$T=\frac{J_{rr'}^{\mathrm{T}}J_{rr'}}{\det(J_{rr'})}\,. \tag{11}$$

Qiu *et al.* [19] classified the geometric transformation functions in terms of the negative (*i.e.*, concave-down) or positive (i.e., concave-up) sign of the second order derivative of this function. The concave-down nonlinear transformation compresses a sphere of radius R_2 in the original space Ω into a shell region $R_1<r'<R_2$ in the compressed space Ω' as

$$r(\beta)=\frac{R_2^{\beta+1}}{R_2^{\beta}-R_1^{\beta}}\left(1-\left(\frac{R_1}{r'}\right)^{\beta}\right), \tag{12}$$

where β denotes the degree of the nonlinearity in the transformation. By taking $\beta\to 0$ in (8), the linear case is obtained, namely

$$r(\beta)=\frac{R_2\mathrm{Ln}(r'/R_1)}{\mathrm{Ln}(R_2/R_1)}\,. \tag{13}$$

All curves belonging to (12) have negative second order derivative with respect to the physical space r'. This class of transformations is termed as the *concave-down* transformation. The transformation function (12) depends on the radial component r' in the spherical coordinate system (r',θ',ϕ').

The concave-up nonlinear transformation compresses a sphere of the radius R_2 in the original space Ω into a shell region $R_1<r'<R_2$ in the compressed space Ω' as

$$r(\beta)=\frac{R_2R_1^{\beta}}{R_2^{\beta}-R_1^{\beta}}\left(\left(\frac{r'}{R_1}\right)^{\beta}-1\right). \tag{14}$$

As $\beta\to 0$, one obtains again the linear case (13). This class of transformations is termed as the *concave-up* transformation because (14) has positive second order derivatives.

3. NUMERICAL RESULTS AND DISCUSSION

In this Section, we illustrate the numerical results obtained using the geometric transformation (10) presented in §2. In the studies below, we suppose that the original domain is a cylinder of radius R_2 and length l, made of an homogeneous and isotropic material. By applying (10), the transformed domain is a shell cylinder of internal and external radii R_1 and R_2, respectively, and of length l'. This domain is made of a new inhomogeneous and anisotropic material.

We begin considering the time-harmonic sound propagation in a medium with density ρ_0 and sound speed c_0 governed by the Helmholtz equation

$$-\rho_0\nabla\cdot\left(\frac{1}{\rho_0}\nabla u(x_1,x_2,x_3)\right)-\kappa^2u(x_1,x_2,x_3)=0\,, \tag{15}$$

where $\kappa = 2\pi f / c_0$ is the wave number, and f is the sound frequency. The cylinder is made of copper ($\rho_0 = 8{,}960$ kg/m^3, $c_0 = 4{,}600$ m/s) and aluminum ($\rho_0 = 2{,}700$ kg/m^3, $c_0 = 6{,}320$ m/s), both materials being considered to be homogeneous and isotropic.

Under a change of coordinates (x', y', z') to (x, y, z) given by (10) with $u'(x_1', x_2', x_3') = J_{x'x}^{-\mathrm{T}} u(x_1, x_2, x_3)$, $J_{x'x} = \dfrac{\partial(x', y', z')}{\partial(x, y, z)}$, Eq. (15) takes the form

$$-\rho'(x_1', x_2', x_3')\nabla \cdot \left(\frac{1}{\rho'(x_1', x_2', x_3')} \nabla u'(x_1', x_2', x_3') \right) - \kappa'(x_1', x_2', x_3')^2 u'(x_1', x_2', x_3') = 0 . \tag{16}$$

The new material is inhomogeneous (the properties are no longer constants but depend on coordinates x_1', x_2', x_3') and anisotropic (tensorial nature) material, whose properties are given by (6):

$$\underline{\underline{\rho}}' = \rho_0 T^{-1}, \quad \underline{\underline{\kappa}}' = \kappa T^{-1}, \tag{17}$$

with T defined by (11) and with the Cartesian basis (x_1, x_2, x_3) defined as $x_1 = r\cos\theta$, $x_2 = r\sin\theta$.

We suppose that the cylindrical specimen has $R_2 = 20$ mm initial radius and $l = 100$ mm initial length. The initial domain is transformed into a shell cylinder with different R_1' and $l' = 80$ mm.

The compression ratio is defined as

$$r_c = \frac{(R_2'^2 - R_1'^2)l'}{R_2^2 l}, \tag{18}$$

where prime $'$ denotes the final parameters. The transformed annulus domain is presented in Fig. 1, for $r_c = 0.152$, 0.35 and 0.6 (the corresponding thicknesses for the annulus $R_1 \le r \le R_2$ are 2 mm, 5 mm and 10 mm, respectively).

Our discussion starts with the computed radial component of the density tensor inside of the shell cylinder for $r_c = 0.152$, 0.35 and 0.6 shown in Fig. 2, for copper and aluminum, respectively. As seen in the figure, the density increases and decreases up to certain values, and starts decreasing again when $r > 9$ mm, for both materials. In conclusion, the density oscillates with respect to the radial coordinate. In order to analyze the properties of the material, let us consider an acoustic pressure field $\mathrm{Re}(u\exp(-2\mathrm{i}\pi ft))$ generated inside of the annulus domain. Fig. 3 illustrates the wave amplitudes u inside and outside of the shell, respectively, for

$r_c = 0.152$ and 0.35. From Fig. 3, one can notice that the wave field inside of the shell (*i.e.* the inner region of radius R_1' which surrounds the acoustic pressure field) is partially isolated from the region situated outside of the shell for $r_c = 0.35$, and is completely isolated from the outside region for $r_c = 0.152$. Actually, the later case corresponds to an acoustic cloak. Obviously, the waves generated inside of the cloak are smoothly confined inside of the inner region of the shell. The inner region is acoustically isolated and the sound is not propagating outside of the shell because the amplitudes on the boundary almost vanish. The domain $r < R_1'$ is an acoustic invisible domain for the exterior observers.

Secondly, we consider the example of the conventional homogeneous and isotropic suspension of fibers characterized by $\rho = 21\ \text{kg/m}^3$. The paper material exhibits several properties similar to foam and soil. As a consequence, the effects of Poison's ratio upon the properties of the material must be analyzed. The Poisson's ratio of the initial material is $\nu = 0.17$. The velocity ratio $\delta = c / c_s$ can be rewritten under the form $\delta^2 = 2(1-\nu)/(1-2\nu)$. Here, c is the longitudinal wave speed, and c_s the transversal wave speed, respectively.

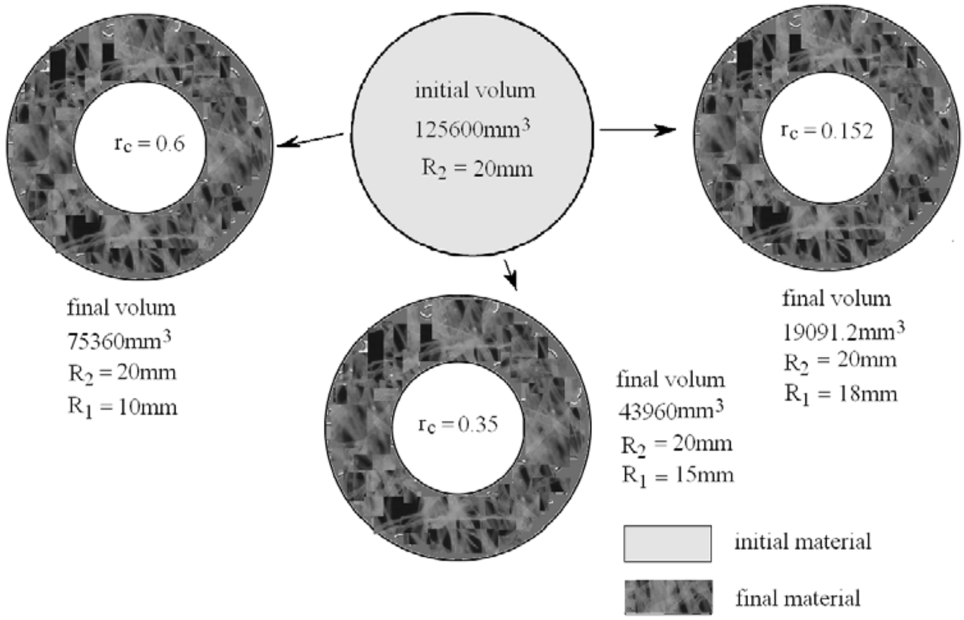

Fig. 1 – Transformed domain.

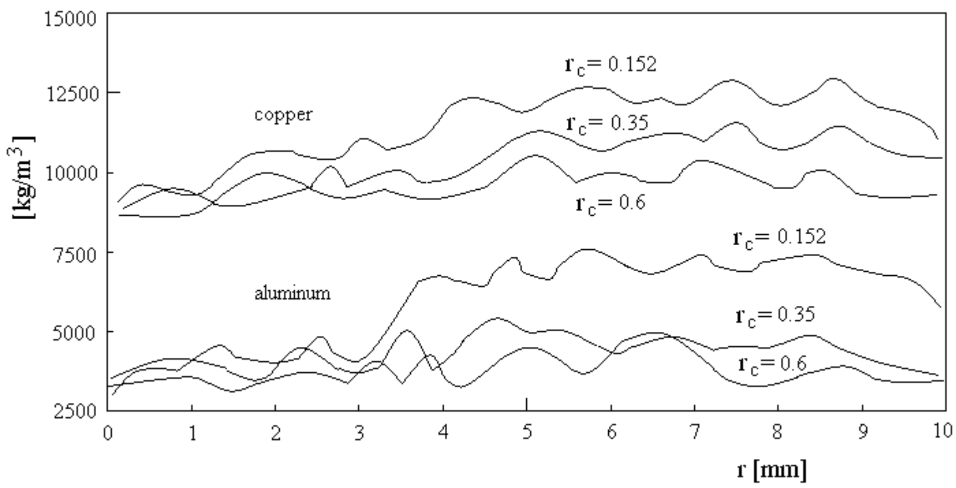

Fig. 2 – Variation of the radial density with respect to radial coordinate.

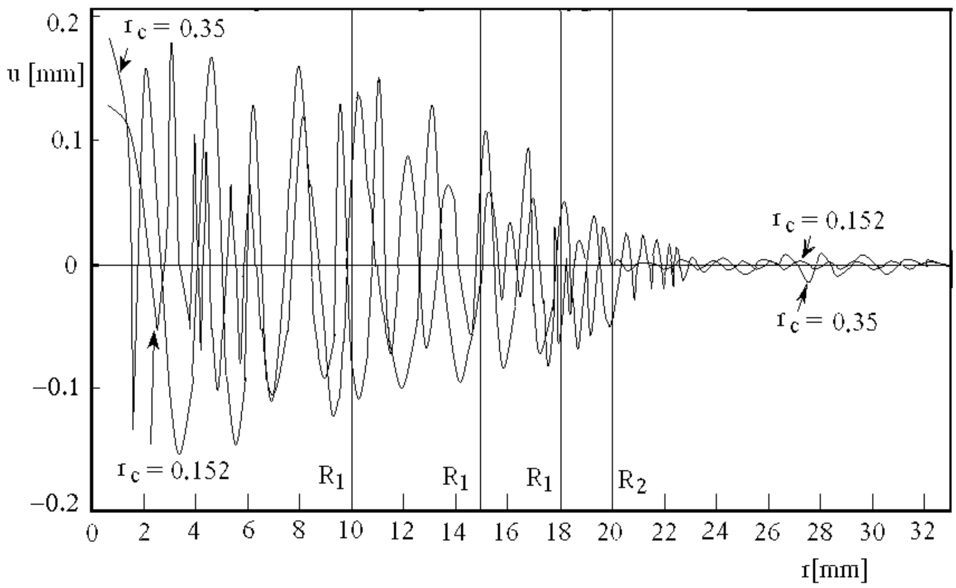

Fig. 3 – Wave field inside and outside of the shell.

Fig. 4 shows the variation of the Poisson's ratio with respect to $1-r_c$ (equivalent to the compressive strain) for the suspension of fibers material (the upper curve) and the paper material (the lower curve) respectively. We observe that the paper material becomes auxetic, *i.e.* a material with negative Poisson's ratio $-0.32<v<0$, for $0.4<1-r_c<0.86$ or $0.14<r_c<0.6$. The auxeticity is related to the property to grow fatter, expanding laterally when stretched instead of getting thinner like an elongated elastic band [10]. Since 1987, when isotropic auxetic foam was manufactured for the first time, negative Poisson's ratio materials have created interest for potential engineering applications. A feature that the auxetic materials showed compared to the other materials is the significant damping capacity which increased up to 16 times compared to the conventional foam material [6, 21].

It seem appropriate to consider, as before, the same initial domain with $R_2 = 20$ mm and $l = 100$ mm, transformed into a shell cylinder with different R_1', $l' = 80$ mm and $r_c = 0.152$, 0.35 and 0.6 (Fig. 1).

Comparing with the case of conventional paper, where the stiffness in the machine direction is usually 1–5 times greater than that in the cross-machine direction, and typically 100 times greater than that in through-thickness direction [22–23, 25–26], the stiffness of the new material has comparable high values for all directions. The variation of the shear stress of the paper material with respect to radial coordinate r is illustrated in Fig. 5, for $r_c = 0.152$, 0.35 and 0.6. The results show that the new material exhibits increased shear strength in comparison to the conventional paper material [24]. The variation of the Young's modulus with respect to radial coordinate $R_1' \le r \le R_2'$ is presented in Fig. 6 for $r_c =$ 0.6 and 0.152 (the corresponding thicknesses for the annulus $R_1 \le r \le R_2$ are 10 mm and 2 mm, respectively). The paper material has increased Young's moduli in all directions in comparison to the conventional paper (30–50 MPa).

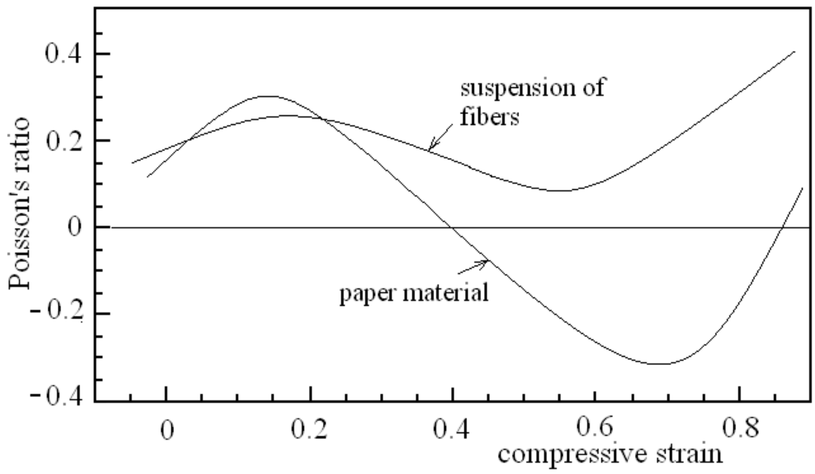

Fig. 4 – Poisson's ratio *versus* compressive strain for suspension of fibers and the conventional paper material.

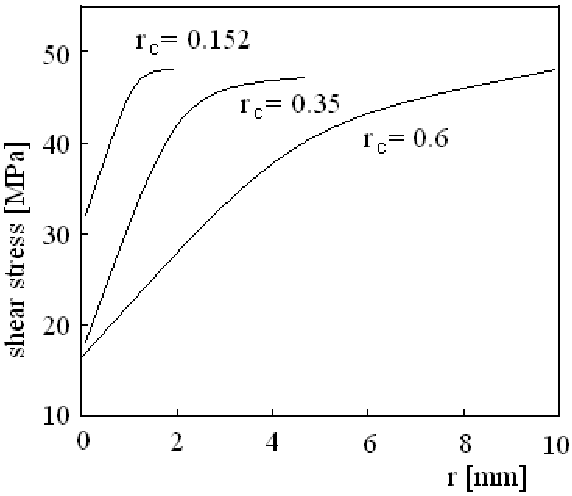

Fig. 5 – Variation of the shear stress with respect to radial coordinate.

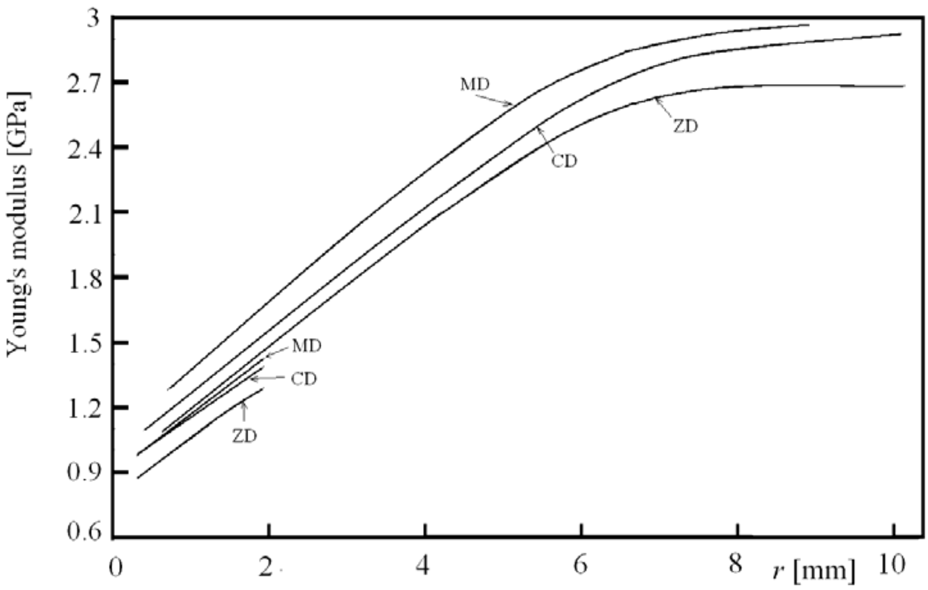

Fig. 6 – Variation of the Young's modulus with respect to radial coordinate.

In the following, we suppose that the transformed annulus domain corresponding to $r_c = 0.152$ (Fig. 1) surrounds a noisy machine, as shown in Fig. 7. By using the wave propagation technique, we show that this domain exhibits the property of a spherical cloak [15].

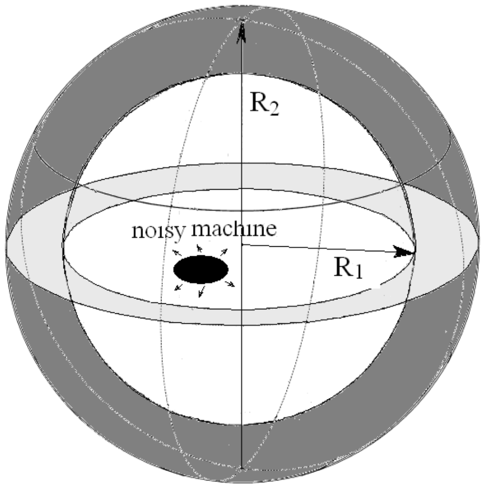

Fig. 7 – Sketch of the spherical cloak surrounding a noisy machine [15].

Fig. 8 illustrates the wave amplitudes u inside and outside of the cloak, respectively, for $r_c = 0.152$. Again, the phenomenon is the same, i.e. the wave field inside of the cloak is completely isolated from the region situated outside of the cloak. One observes that the inner region is acoustically isolated and the sound is not detectable by an exterior observer because the amplitudes on the boundary vanish. For these particular cases, it is easy to imagine an object invisible to sound by building a box around it to prevent the wave from reaching the object.

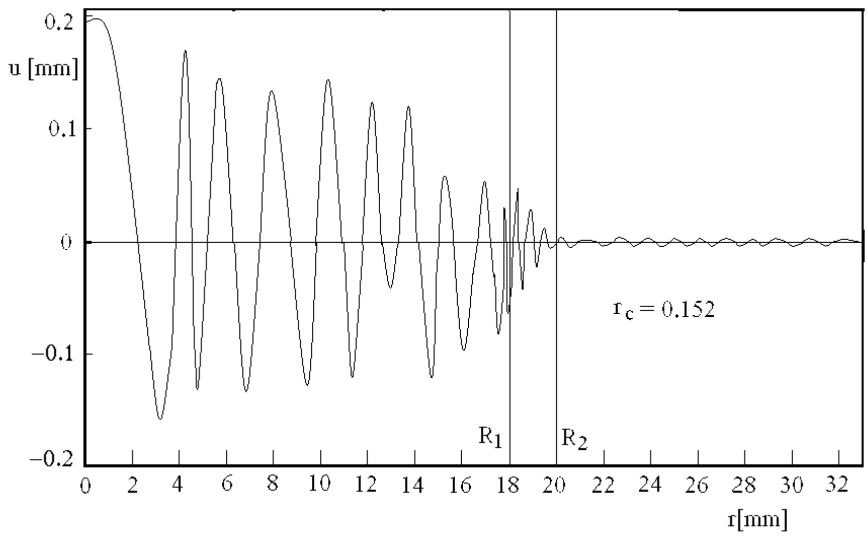

Fig. 8 – Wave fields inside and outside of the cloak.

4. CONCLUDING REMARKS

The idea for transforming homogeneous and isotropic materials into new materials is the main goal of this paper. The property of Helmholtz equation to be invariant under geometric transformations is exploited in order to transform an original cylinder made of an initial material, into a shell cylinder made of a new inhomogeneous and anisotropic material.

The results show that the new materials can cloak regions of space, making them invisible to sound. We refer to acoustic cloaking which occurs when a medium contains a region in which noisy objects can be acoustically hidden.

In conclusion, geometric transformations can be used in designing new materials [29]. By manipulating the spatial compression, different performances can be achieved under inhomogeneous and anisotropic materials that might be useful in the design of elastic cloaking devices.

Acknowledgements. This research was financially supported by the National Authority for Scientific Research (ANCS, UEFISCSU), Romania, through project PN-II nr. 745/2009, code ID_1391/2008.

Received on August 25, 2011

REFERENCES

1. ALÙ, A., ENGHETA, N., *Achieving transparency with plasmonic and metamaterial coatings*, Physical Revue E, **72,** *1*, Paper 016623 (9 pages), 2005.
2. BIGONI, D., SERKOV, S.K., VALENTINI, M., MOVCHAN, A.B., *Asymptotic models of dilute composites with imperfectly bonded inclusions*, International Journal of Solids and Structures, **35**, *24*, pp. 3239-3258, 1998.
3. BRUN, M., GUENNEAU, S., MOVCHAN, A.B., *Achieving control of in-plane elastic waves*, Applied Physics Letters, **94**, *6*, Paper 061903 (3 pages), 2009.
4. CUMMER, S.A., POPA, B.I., SCHURIG, D., SMITH, D.R., PENDRY, J., RAHM, M., STARR, A., *Scattering theory derivation of a 3D acoustic cloaking shell*, Physical Review Letters, **100,** *2*, Paper 024301 (4 pages), 2008.
5. CUMMER, S.A., SCHURIG, D., *One path to acoustic cloaking*, New Journal of Physics, **9**, *3*, Paper 045, 2007.
6. DONESCU, Şt., CHIROIU, V., MUNTEANU, L. *On the Young's modulus of an auxetic composite structure*, Mechanics Research Communications, **36**, *3*, pp. 294-301, 2009.
7. DUPONT, G., FARHAT, M., DIATTA, A., GUENNEAU, S., ENOCH, S., *Numerical analysis of three-dimensional acoustic cloaks and carpets*, Wave Motion, **48**, *6*, pp. 483-496, 2011.
8. GREENLEAF, A., LASSAS, M., UHLMANN, G., *On nonuniqueness for Calderón's inverse problem*, Mathematical Research Letters, **10**, *5*, pp. 685-693, 2003.
9. GUENNEAU, S., McPHEDRAN, R.C., ENOCH, S., MOVCHAN, A.B., FARHAT, M., NICOROVICI, N.A., *The colours of cloaks*, Journal of Optics, **13**, *2*, paper 024014, 2011.
10. LAKES, R.S., *Experimental micro mechanics methods for conventional and negative Poisson's ratio cellular solids as Cosserat continua*, Journal of Engineering Materials and Technology, **113**, *1*, pp. 148-155, 1991.
11. LEONHARDT, U., *Optical conformal mapping*, Science, **312**, pp. 1777-1780, 2006.

12. MILTON, G.W., NICOROVICI, N.-A., *On the cloaking effects associated with anomalous localized resonance*, Proceedings of the Royal Society A, **462**, pp. 3027-3059, 2006.
13. MILTON, G.W., *New metamaterials with macroscopic behavior outside that of continuum elastodynamics*, New Journal of Physics, **9**, Paper 359 (13 pages), 2007.
14. MILTON, G.W., BRIANE, M., WILLIS, J.R., *On cloaking for elasticity and physical equations with a transformation invariant form*, New Journal of Physics, **8**, Paper 248 (20 pages), 2006.
15. MUNTEANU, L., CHIROIU, V., *On the three-dimensional spherical acoustic cloaking*, New Journal of Physics, 13, 8, 083031, 2011.
16. NORRIS, A.N., *Acoustic cloaking theory*, Proceedings of the Royal Society A, **464,** pp. 2411-2434, 2008.
17. NORRIS, A.N., SHUVALOV, A.L., *Elastic cloaking theory*, Wave Motion, **48**, *6*, pp. 525-538, 2011.
18. PENDRY, J.B., SHURIG, D., SMITH, D.R., *Controlling electromagnetic fields*, Science, **312,** pp. 1780-1782, 2006.
19. QIU, C.W., HU, L., ZHANG, B., WU, B.I., JOHNSON, S.G., JOANNOPOULOS, J.D. *Spherical cloaking using nonlinear transformations for improved segmentation into concentric isotropic coatings*, Optics Express, **17**, *16*, pp. 13467-13478, 2009.
20. RODAL, J.J.A., *Paper deformation in a calendering nip*, Proceedings of the 1993 TAPPI Finishing and Converting Conference, New Orleans, USA, pp. 321-349, 1993.
21. SCARPA, F., CIFFO, L.G., YATES, J.R., *Dynamic properties of high structural integrity auxetic open cell foam*, Smart Materials and Structures, **13**, pp. 49-56, 2004.
22. STENBERG, N., *Out-of-plane shear of paperboard under high compressive loads*, Journal of Pulp and Paper Science, **30**, *1*, pp. 22-28, 2004.
23. STENBERG, N., FELLERS, C., *The out-of-plane Poisson's ratios of paper and paperboard*, Nordic Pulp and Paper Research Journal, **17**, *4*, pp. 387-394, 2003.
24. STENBERG, N., *A model for the through-thickness elastic-plastic behavior of paper*, International Journal of Solids and Structures, **40**, *26*, pp. 7483-7498, 2003.
25. STENBERG, N., FELLERS, C., ÖSTLUND, S., *Measuring the stress-strain properties of paperboard in the thickness direction*, Journal of Pulp and Paper Science, **27**, *6*, pp. 213-221, 2001.
26. STENBERG, N., FELLERS, C., ÖSTLUND, S., *Plasticity in the thickness direction of paperboard under combined shear and normal loading*, Journal of Engineering Materials and Technology, **123**, *2*, pp. 184-190, 2001.
27. VASQUEZ, F.G., MILTON, G.W., ONOFREI, D., SEPPECHER, P., *Transformation elastodynamics and active exterior acoustic cloaking*, Submitted as a chapter in: *Acoustic metamaterials: Negative refraction, imaging, lensing and cloaking*, eds. Craster and Guenneau, Springer, 2011.
28. ZOLLA, F., GUENNEAU, S., NICOLET, A., PENDRY, J.B, *Electromagnetic analysis of cylindrical invisibility cloaks and the mirage effect*, Optics Letters, **32**, *9*, pp. 1069-1071, 2007.
29. CHIROIU, V., TEODORESCU, P.P., MUNTEANU, L., *On the geometric transformations and auxetic materials*, Analele Universității "Eftimie Murgu" Reşiţa, Anul XVIII, *1*, pp. 73-82, 2011.